Computational Sciences and Engineering 3(2) (2023) 201-211

University of Guilan

Computational Sciences and Engineering

journal homepage: https://cse.guilan.ac.ir/

A low-power sixth-order Gm-C low-pass filter usable in audio applications

Mohsen Ghaemmaghami [a], Shahbaz Reyhani [a,*]

[a] Department of Electrical Engineering, University of Guilan, Persian Gulf Highway, Rasht, 41996-13776, Iran

ARTICLE INFO

Article history:
Received 10 May 2024
Received in revised form 13 June 2024
Accepted 15 June 2024
Available online 15 June 2024

Keywords:
Active filter
Tunable low-pass filter
Analog to Digital Converter
Digital to Analog Converter
Gm-C low-power filter

ABSTRACT

This paper presents a Gm-C tunable sixth-order active low-pass filter designed using an operational transconductance amplifier (OTA) that can be utilized at the front-end of analog to digital converters (ADCs) or to be used in the output of digital to analog converters (DAC). The tunable filter is used to match its cutoff frequency with the bandwidth of ADC and DAC. The proposed tunable low-pass sixth-order filter is designed and simulated in 180 nm CMOS technology at the transistor level. The simulation results show that by changing the three bias voltages in the proposed filter at the range of 0.2 V to 0.4 V, its bandwidth changes between 4 KHz and 20 KHz. The maximum attenuation of unwanted signals outside the bandwidth is 85 dB. The power consumption of the designed filter is equal to 623 μW at the supply voltage of 1.8 V.

1. Introduction

The audio signals include a set of information that play an important role in everyday communication. Humans have the ability to receive and process sound vibrations in the range of 20 Hz to 20 kHz. Today, the need for image and speech processing has increased, and so far many advances have been made in this field [1]. In order to process the audio signal, it is necessary to convert it into digital information, which can be used with an ADC [2]. The ADCs are electronic circuits that convert continuous analog signals to discrete digital data for processing and storage [3].

One of the important applications of ADCs is their use in communication devices, biomedical applications, image and audio processing [4-7]. ***Figure 1*** shows the process of converting the analog signal to digital codes and then reconstructing the processed signal.

* Corresponding author.
E-mail addresses: shahbaz@guilan.ac.ir (Sh. Reyhani)

https://doi.org/10.22124/cse.2024.27437.1077

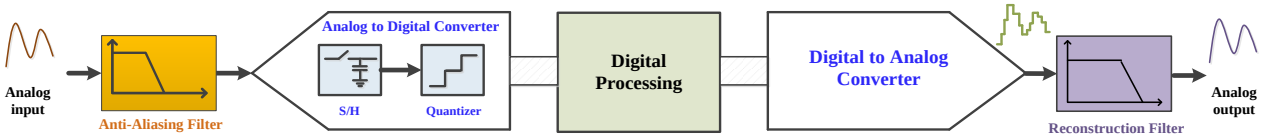

Figure 1. Application of ADC and DAC: conversion of the analog signal to digital codes, processing the digital data and reconstructing the digital audio from the processed data.

To convert an analog signal to digital codes, first the analog signal is passed through the anti-aliasing filter to prevent unwanted signals from entering the converter in order not to reduce the ADC performance [8]. The output of the anti-aliasing filter is sampled by the sample and hold (S/H) circuit and the quantizer produces the corresponding digital code according to the voltage level of each samples [3]. On the other hand, after processing the digital codes, it is possible to converting them to the analog signal using a DAC. The DAC output can be smoothed using a reconstruction filter. It is necessary to be adjusted the bandwidth of the used filters according to the bandwidth of the ADC and DAC, thus the tunable filters will be needed.

The design of passive filters consisting of resistors, inductors and capacitors in the frequency range of 1 Hz to 1 MHz is not practical to integration due to the high area consumption, and the integrated active filters are used for this frequency range [9-11]. One of the common structures in the design of active filters is the Gm-C structure, which has features such as relatively high stability, integration capability, optimal power consumption, and the ability to be adjusted in different frequency ranges [12].

In this article, a sixth-order tunable low-pass filter is presented, which can be used in audio applications. In the second part of this article, the structure of the proposed Gm-C filter will be presented along with the analysis of the relevant circuits, and also the operation of the proposed circuit will be explained. In the third part, simulation results will be reported, and the fourth part is the conclusion of the article.

2. Structure of the proposed Gm-C low-pass filter

The block diagram of the proposed tunable sixth-order low-pass filter is shown in ***Figure 2***. The proposed filter consists of three cascaded second-order low-pass filter stages. The cutoff frequencies of the proposed filter can be tuned using the bias voltages of OTAs for audio frequency applications.

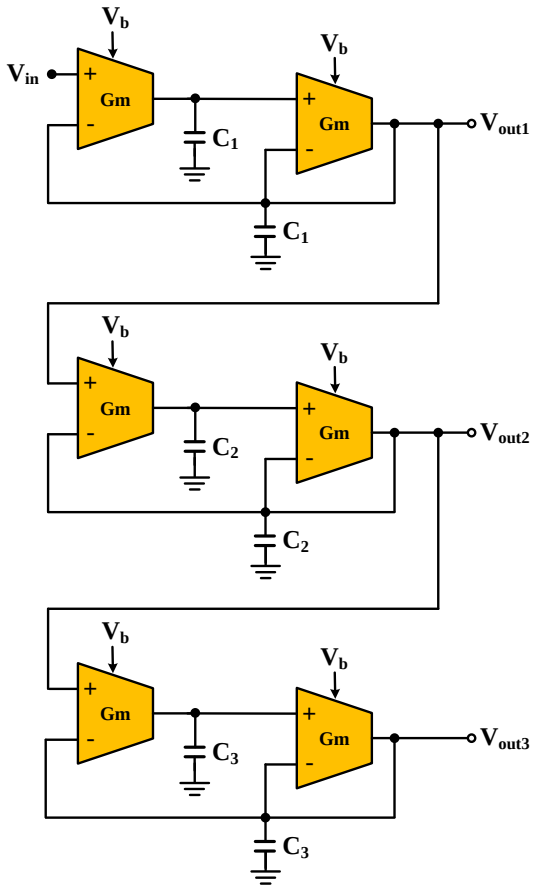

Figure 2. The structure of the proposed sixth-order low-pass filter.

2.1. Analysis of the proposed second-order Gm-C filter

In order to simplify the description of the operation of the proposed filter, first a second-order low-pass circuit is analyzed. The schematic of the proposed second-order is shown in ***Figure 3***.

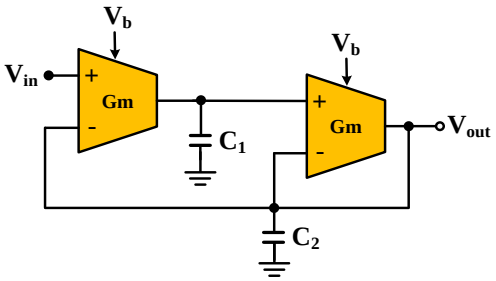

Figure 3. The schematic of second-order low-pass filter circuit with tunable capability.

The transconductance amplifiers are actually known as differential voltage controlled current source. Their g_m value is calculated from ***Eq. (1)***.

$$g_m = \frac{I_{out}}{V_{in}} \quad \textbf{(1)}$$

Where I_{out} indicates the output current and V_{in} is the input voltage. The g_m can be considered as a main parameter in the design of an active filter and can usually be adjusted with a bias current (I_{bias}) in the transconductance amplifier. The tunability in analog integrated circuits is one of the

important features that is considered today due to the tolerance of the fabricated parts [13]. The transfer function of the proposed Gm-C filter shows the dependence of its cutoff frequency on the transconductance of the amplifiers. The transfer function of the second-order low-pass filter is shown in ***Eq. (2)***.

$$TF = \frac{g_{m1}g_{m2}}{S^2C_1C_2 + SC_1g_{m1} + g_{m1}g_{m2}} \quad \textbf{(2)}$$

Where g_{m1} and g_{m2} are transconductance of the first and second amplifiers and C_1 and C_2 are the capacitance of capacitors used in the proposed circuit. Assuming that the transconductance of the OTAs and the capacitance of the capacitors are equal, the cutoff frequency of the low-pass filter (ω_0) is obtained from ***Eq. (3)***.

$$\omega_0 = \frac{g_m}{\sqrt{c_1c_2}} \quad \textbf{(3)}$$

It can be seen from ***Eq. (1)*** that the transconductance of the amplifiers can be changed only by changing the bias voltage of the circuit, so the cutoff frequency of the desired filter can be tuned using the bias voltage applied to the amplifiers. The frequency response of the second-order low-pass filter is shown in ***Figure 4***. By changing the bias voltage in the range of 0.2-0.4 V, the cutoff frequency in the desired filter is tuned between 4 kHz and 20 kHz. The capacitance of C1 and C2 capacitor capacitors are 4pF and 4.8pF, respectively.

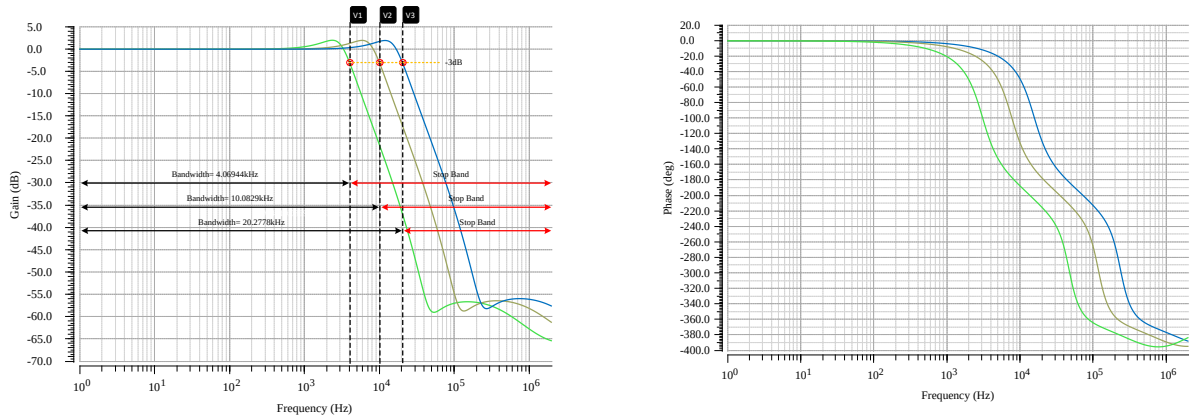

(a) (b)

Figure 4. The frequency response of the proposed second-order low-pass filter (a) Gain (b) Phase.

2.2. Proposed operational transconductance amplifier

The schematic of the transconductance amplifier used in the designed low-pass filter is shown in ***Figure 5***. The transconductance value in the proposed OTA can be adjusted by the bias voltage (V_b).

The proposed differential transconductance amplifier has an output gain of 91 dB, a bandwidth of 6.8 MHz, a phase margin of 70 degrees, and a common mode rejection ratio (CMRR) of 105 dB. ***Figure 6*** shows the gain and phase diagram of the designed amplifier. ***Table 1*** shows the size of the transistors used in the proposed amplifier, the currents and transconductance of each transistor.

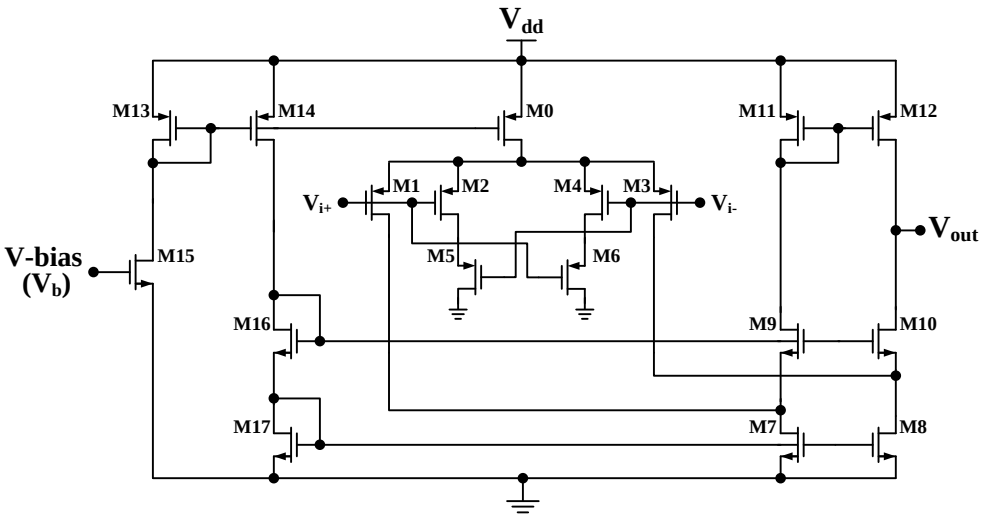

Figure 5. The schematic of the proposed OTA circuit with the ability to adjust transconductance.

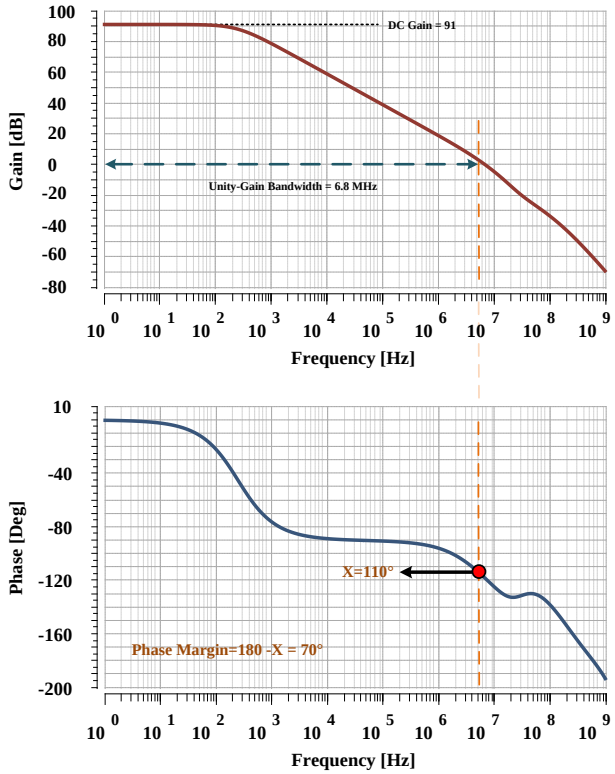

Figure 6. The frequency responses of the proposed OTA for V_b = 0.6V (gain and phase response).

Table 1. The sizing of the transistors used in the proposed OTA.

Transistor	W(μm)	L(μm)	M	I_d(μA)	g_m(μS)
M_0	4	2	7	6.15	83.5
M_1, M_3	2	2	6	1	31.5
M_2, M_4	2	2	6	2.1	11.1
M_5, M_6	2	2	6	2.1	18
M_7, M_8	5.2	2	3	4.74	77.5
M_9	5.2	2	1	2.7	37.8
M_{10}	5.2	2	1	2.7	38.2
M_{11}, M_{12}	4	2	7	2.7	45.7
M_{13}, M_{14}	4	2	7	6.2	84.5
M_{15}	25.2	2	2	6.2	83
M_{16}, M_{17}	2	2	5	6.2	102

2.2. Structure of the proposed Gm-C low-pass filter

The tunable Gm-C sixth-order low-pass filter circuit using three stages of the second-order low-pass filter is shown in ***Figure 7***. The cutoff frequency of the filter can be set in a desired frequency by changing the bias voltages of the amplifiers. In the proposed low-pass filter circuit, the capacitance of the MIM capacitors are 4 pF and 4.8 pF.

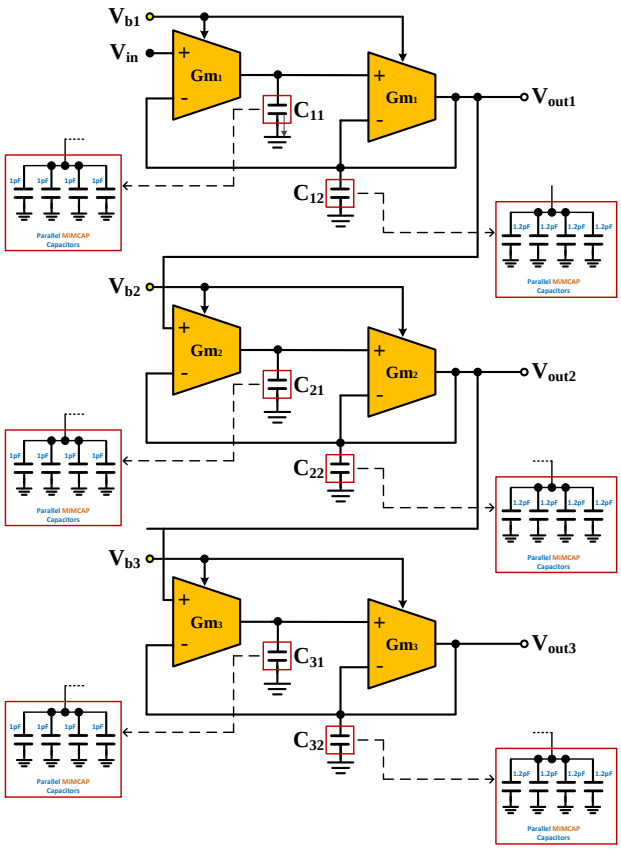

Figure 7. The schematic of proposed tunable sixth-order low-pass filter.

3. Simulation results

The proposed low-pass filter proposed is designed and simulated at the transistor level as a schematic and layout in 180 nm CMOS technology. In order to consider the ability to tune the cutoff frequency of the proposed filter by adjusting the bias voltages, the simulation results of the proposed filter are presented at two levels of pre-layout and post-layout design.

3.1. Pre-layout simulation results

In this section, the effect of adjusting the bias voltages on the cutoff frequency of the proposed filter is investigated. The frequency responses of the designed low-pass filter are shown ***Figure 8***. As shown in ***Figure 8***, the bandwidth of the proposed filter can be adjusted by changing the bias voltages. The amounts of attenuation for all three cutoff frequencies of 4 KHz, 10 KHz and 20 KHz are 169 dB 169 dB and 168 dB, respectively. The multiple simulation results are presented in ***Table 2***.

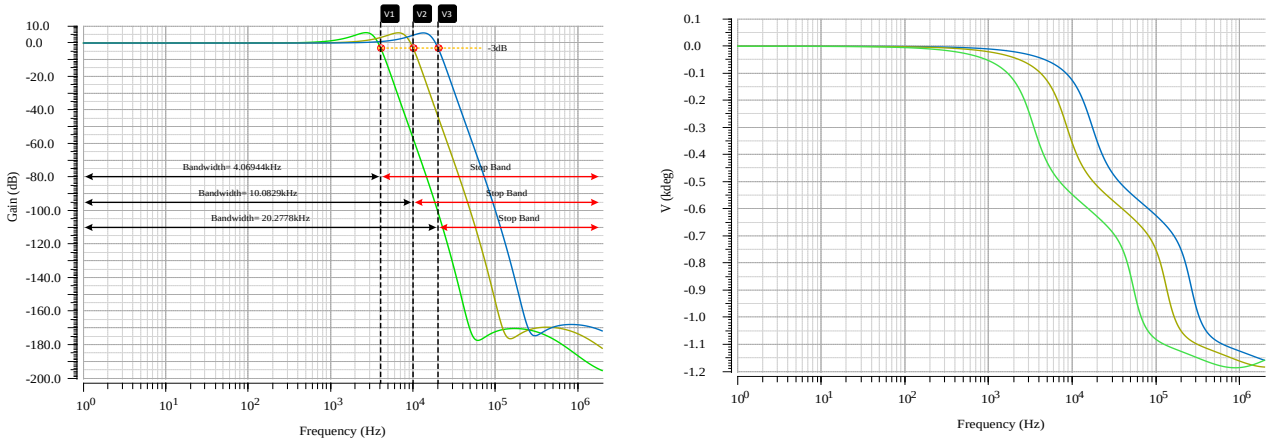

(a) (b)

Figure 8. The frequency responses of the proposed filter for the cutoff frequencies of 4 KHz, 10 KHz, and 20 KHz (a) gain (b) phase.

Table 2. The specifications of the proposed filter obtained from the pre-layout simulation: bias voltages of each stage, cutoff frequency and attenuation at start of stop-band.

Audio application	Bias Voltage1(V)	Bias Voltage2(V)	Bias Voltage3(V)	Cut-off Frequency (KHz)	Maximum attenuation (dB)
Telephone	0.2	0.21	0.22	4	169
Speech	0.3	0.34	0.31	10	169
Music	0.4	0.39	0.36	20	168

Also, the frequency responses of the proposed low-pass filter with all of the 2nd, 4th and 6th orders for the bandwidth of 20 kHz are shown in ***Figure 9***. It is clear that as the order of the filter increases, its attenuation and slope increase by a factor of two.

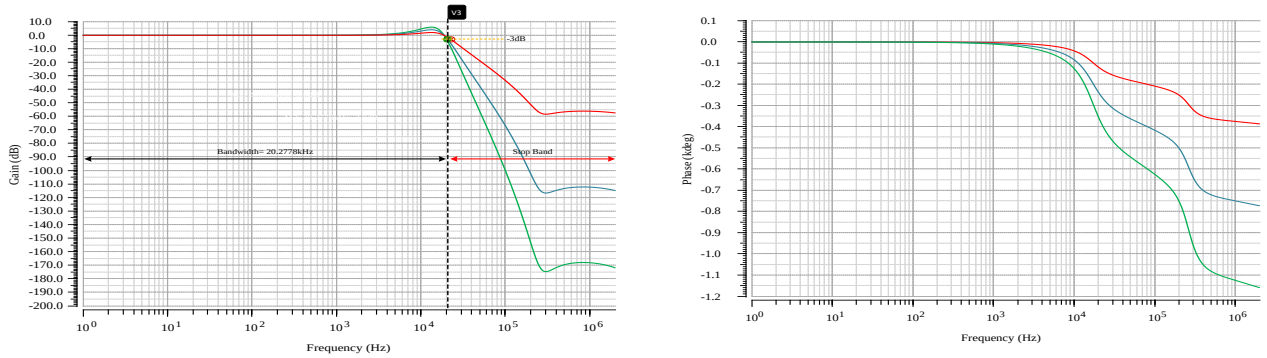

(a) (b)

Figure 9. The frequency responses of the proposed 2nd, 4th and 6th order low-pass filter (a) gain (b) phase.

In order to determine the performance of the proposed circuit more precisely, especially the mismatch of the used devices, Monte Carlo analysis has been performed on +/- %2 deviation in the capacitance of the capacitors and the input transistors of the transconductance amplifiers for 1000 iterations. According to the obtained results, the designed filter has the low sensitivity against the mismatch of the components. As shown in the histograms of ***Figure 10***, despite the mismatch in the components used in the designed circuit, the cutoff frequencies of the proposed filter have very little deviation.

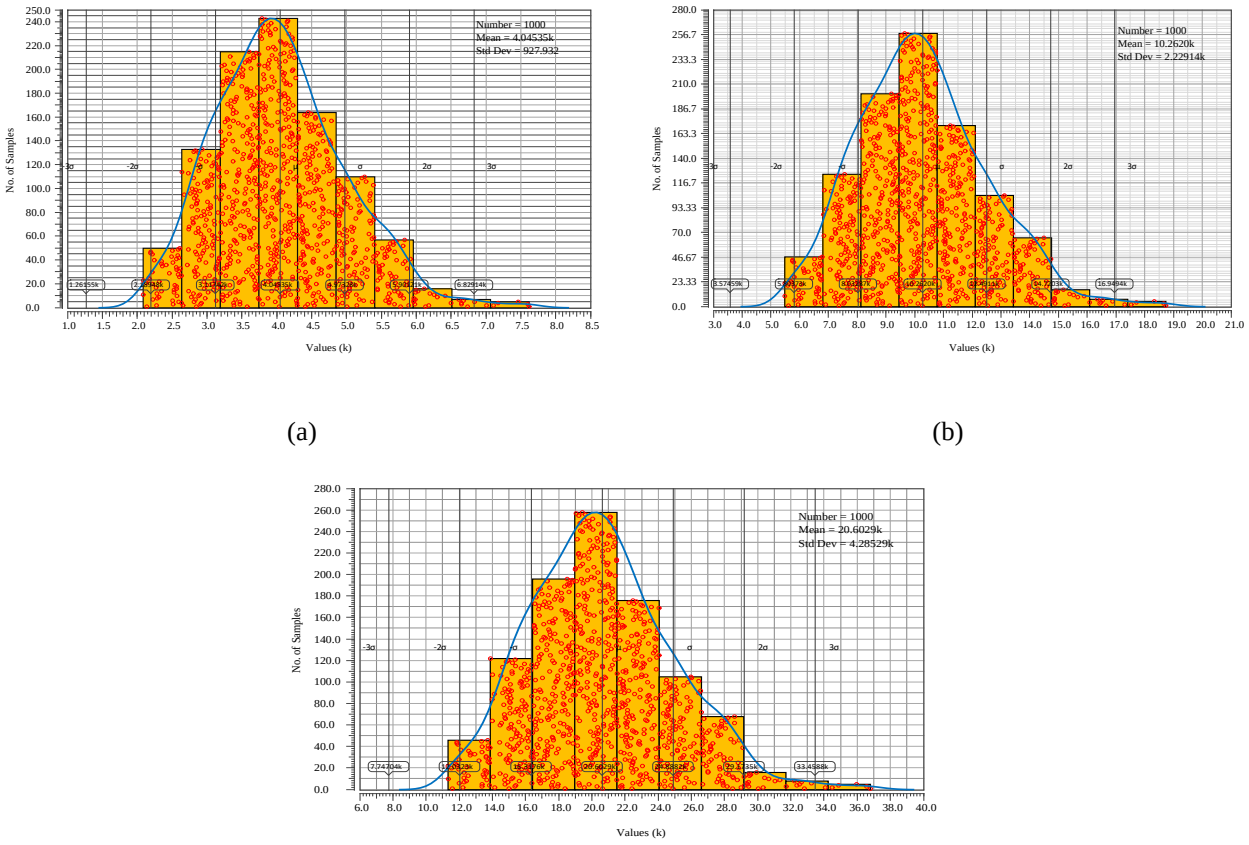

(a) (b)

(c)

Figure 10. The histograms of Monte Carlo analysis on the proposed filter for cutoff frequencies: (a) 4 kHz (b) 10 kHz (c) 20 kHz.

3.2. Post-layout Simulation results

The layout of the proposed low-pass filter is shown in ***Figure 11***. This arrangement has dimensions of 373 µm x 361 µm, which occupies an area equal to 0.135 mm^2 of the chip surface. The frequency response related to the post-layout simulation for audio bandwidth is given in ***Figure 12***. The simulation results show the difference between the two frequency responses at the schematic level and post-layout in the amount of stop-band attenuation. The attenuation of the designed filter in the post-layout simulation has decreased compared to the schematic level, which is due to the presence of parasitic elements. The presence of parasitic capacitors and resistors during the post-layout simulation reduces the performance of circuits. The main feature of the proposed filter is that the cutoff frequency of the filter does not changed in the post-layout simulation and the stability of the circuit is still well maintained. The simulation results are presented in ***Table 3***. ***Table 4*** shows the comparison of proposed filter with state-of-the-art low-pass active filters.

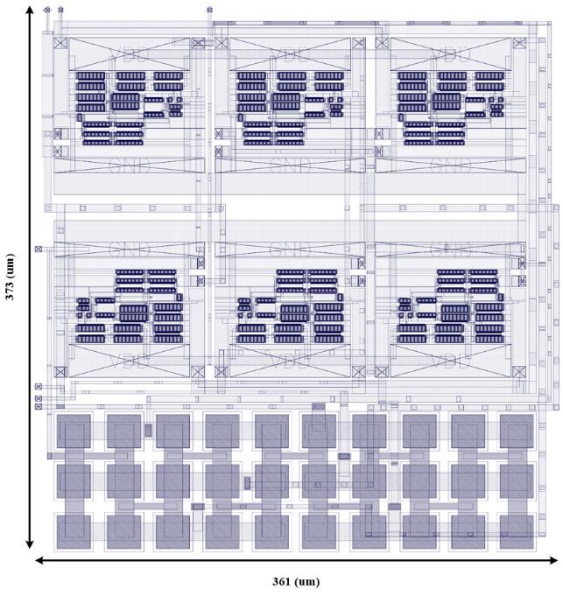

Figure 11. The layout of the proposed sixth-order low-pass filter.

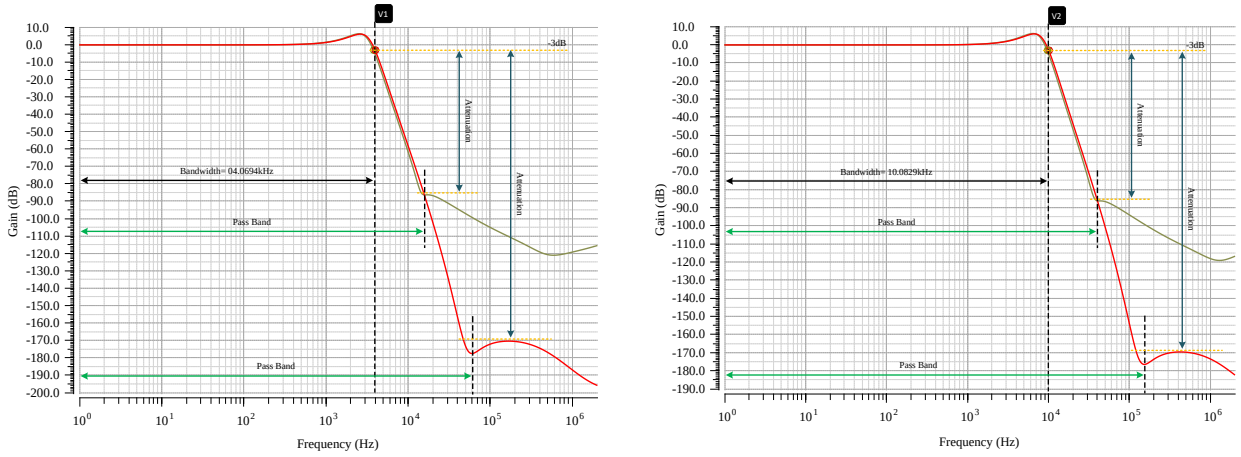

(a) (b)

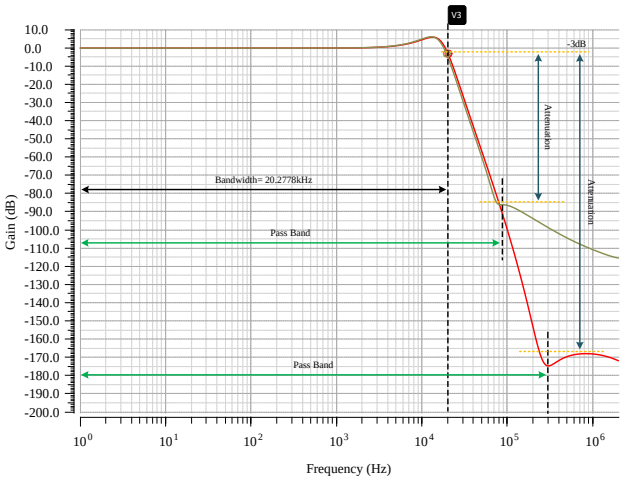

(c)

Figure 12. The Frequency responses of the pre-layout and post-layout simulations: (a) 4 kHz (b) 10 kHz (c) 20 kHz.

Table 3. The specifications of the proposed filter obtained from the post-layout simulation: bias voltages of each stage, cutoff frequency and attenuation at start of stop-band.

Audio application	Bias Voltage1(V)	Bias Voltage2(V)	Bias Voltage3(V)	Cut-off Frequency (KHz)	Maximum attenuation (dB)
Phone	0.2	0.21	0.22	4	85
Speech	0.3	0.34	0.31	10	85
Music	0.4	0.39	0.36	20	85

Table 4. Comparison of the performance of the proposed filter with previous works.

Designed filters	Technology (nm)	Filter order	supply voltage (V)	The number of capacitors	Cutoff Frequency (KHz)	power consumption (mW)	Area (mm^2)
This work	180	6	1.8	24	4-20	0.062	0.135
[14]	90	4	1.2	11	0.114-12000	11.83	N/A
[15]	180	2	1.8	4	100	0.258	0.1452
[16]	350	2	2.5	6	30	1.3	0.465

4. Conclusion

The sixth-order low-pass filter is designed using Gm-C type cascade structure, which has the ability to tune the cutoff frequency of 4 KHz, 10 KHz and 20 KHz. The proposed filter is designed and simulated at the transistor level in 180 nm CMOS technology. The presented low-pass filter can be used as an anti-aliasing filter before the ADCs or a reconstruction filter after the DACs in audio applications. It will be possible to adjust the cutoff frequencies of the proposed filter for use in the desired frequency range by changing the three bias voltages. The simulation results showed that the cutoff frequency of the designed filter can be set in the range of 4 kHz to 20 kHz by

adjusting the bias voltages between 0.2 V to 0.4 V. The power consumption of the proposed filter is equal to 623 μW at the supply voltage of 1.8 V. The attenuation in stop-band of the designed low-pass filter is 85 dB.

References

[1] Umapathy, K., Ghoraani, B., & Krishnan, S. (2010). Audio signal processing using time-frequency approaches: coding, classification, fingerprinting, and watermarking. *EURASIP Journal on Advances in Signal Processing*, 2010, 1-28.

[2] Zheng, Y., Zhao, Y., Zhou, N., Wang, H., & Jiang, D. (2021). A short review of some analog to digital converters resolution enhancement methods. *Measurement*, 180, 109554.

[3] Maloberti, F. (2007). *Data converters specifications*, 47-76. Springer US.

[4] Sundarasaradula, Y., Constandinou, T. G., & Thanachayanont, A. (2016, December). A 6-bit, two-step, successive approximation logarithmic ADC for biomedical applications. In *2016 IEEE International Conference on Electronics, Circuits and Systems (ICECS)*, 25-28. IEEE.

[5] Thirrunavukkarasu, R. R., Kirthika, S., Nivetha, N., & Renuka, N. (2019, March). Design of Sar-Adc based mixed signal architecture for low power application. In *2019 5th International Conference on Advanced Computing & Communication Systems (ICACCS)*, 822-824. IEEE.

[6] Lee, T. Y., Butcher, T., Ishida, T., Panigada, A., & Meacham, D. (2017, March). Digitally enhanced high speed ADC for low power wireless applications. In *2017 IEEE MTT-S International Conference on Microwaves for Intelligent Mobility (ICMIM)*, 64-67. IEEE.

[7] Judy, M., Sodagar, A. M., Lotfi, R., & Sawan, M. (2013). Nonlinear signal-specific ADC for efficient neural recording in brain-machine interfaces. *IEEE transactions on Biomedical Circuits and Systems*, 8(3), 371-381.

[8] Chen, H. W., Lee, S., & Flynn, M. P. (2023). An Anti-Aliasing-Filter-Assisted 3rd-Order VCO-Based CTDSM With NS-SAR Quantizer. *IEEE Journal of Solid-State Circuits*.

[9] Yesil, A., Yuce, E., & Minaei, S. (2018). Inverting voltage buffer based lossless grounded inductor simulators. *AEU-International Journal of Electronics and Communications*, 83, 131-137.

[10] Mohammad, F., Sampe, J., Shireen, S., & Ali, S. H. M. (2017). Minimum passive components based lossy and lossless inductor simulators employing a new active block. *AEU-International Journal of Electronics and Communications, 82*, 226-240.

[11] Kaçar, F., Yeşil, A., Minaei, S., & Kuntman, H. (2014). Positive/negative lossy/lossless grounded inductance simulators employing single VDCC and only two passive elements. *AEU-International Journal of Electronics and Communications*, *68*(1), 73-78.

[12] Başak, M. E. (2019). Realization of DTMOS based CFTA and multiple input single output biquadratic filter application. *AEU-International Journal of Electronics and Communications*, *106*, 57-66.

[13] Gu, Q. (2015). *RF tunable devices and subsystems: Methods of modeling, analysis, and applications*. Cham, Switzerland: Springer International Publishing.

[14] Elamien, M. B., & Mahmoud, S. A. (2018). An 114 Hz–12 MHz digitally controlled low-pass filter for biomedical and wireless applications. *IET Circuits, Devices & Systems*, *12*(5), 606-614.

[15] Kumar, T. B., Kar, S. K., & Boolchandani, D. (2020). A wide linear range CMOS OTA and its application in continuous-time filters. *Analog Integrated Circuits and Signal Processing*, *103*(2), 283-290.

[16] Soares, C. F., de Moraes, G. S., & Petraglia, A. (2014). A low-transconductance OTA with improved linearity suitable for low-frequency Gm-C filters. *Microelectronics Journal*, *45*(11), 1499-1507.